THE DEMONSTRATION OF A SYSTEM TO ANALYSE THE TEMPERATURE DEPENDENCE OF CONDENSED MATTER PHENOMENA.

A dissertation submitted in partial fulfilment of the requirements for the Masters in Physics

by Samuel Wright

Department of Physics, University of Oxford

23rd April 2012

Supervisor: Professor Robin Nicholas

Word Count: 6262

Abstract

We prescribe a software package and analytical method to capture, analyse and interpret photoluminescence and transmission spectra of a sample in the visible range, and apply this method to a variety of samples (crystalline and polymer semiconductors, and a variety of multi-quantum wells) to observe changes in energy gaps and phonon energies as a function of temperature, then discuss the principles behind the observations.

1 Introduction

Transmission and photoluminescence (PL) spectra provide an understanding of the energetics of electron excitation and relaxation respectively, providing an insight into the structure and dynamics found inside a material. This can be used to then understand the underlying physical phenomena that give rise to these dynamics.

This paper starts with an overview of the relevant condensed matter phenomena that we will be studying, and how they might depend on the sample's temperature. We then present data from a variety of samples showing the temperature dependence of PL spectra peaks and transmission spectra edges, before discussing their physical relevance in the context of the topics discussed in section 2.

The appendix is a lab script that a physics undergraduate could follow in order to showcase the phenomena described in this paper. It demonstrates how to use the software and tools we developed to collect and analyse data. Our hope is that this will be introduced into the undergraduate practical teaching course at Oxford University.

2 Overview Relevant Physical Phenomena

2.1 Semiconductors

A key property of a semiconductor is that a small yet finite gap exists between the highest-energy occupied electron state and the lowest-energy unoccupied electron state. This gap can have the energy of a visible-range photon, so a visible-light source can be used to excite outer electrons to transition between these states, then a visible-light spectrometer can be used to measure transmission or PL from the material. It is the ease with which electron transitions can be controlled which makes semiconductors ideal for this experiment, since we can be certain that we are only activating one transition. This would be in contrast to, for example, X-ray spectrometry which would activate a variety of transitions and could complicate data analysis.

Crystalline Semiconductors

In a crystalline semiconductor, the electrons occupy delocalised wavefunctions which are distributed throughout the material. These wavefunctions are similar to a free-electron wavefunction because (semi-classically) a nucleus on an electron's left will attract it almost as much as the nucleus on its right. Putting a free-particle in an infinite-potential well and applying the relevant boundary condition is all that's required to quantise the possible wavefunctions - similarly, putting a free-electron in a periodic potential applies a condition on the available wavefunctions which leads to quantisation. It is slightly different here since the potential is weak instead of infinite (so the electrons retain a free-electron-like wavefunction) and the boundary condition is periodic instead of being confined to a well (so the allowed k-states relate to having the wavefunction match up to the lattice structure). Similar k-states of different magnitude form a continuous band of states, which can have a finite difference in energy to other bands known as the band gap energy. In a semiconductive crystal this is a few eV and so the electrons in the highest-energy band will be excited by visible-light photons.

Temperature of the material will most affect its band gap by thermal expansion of the lattice, equating to thermal shrinking of the reciprocal lattice and a decrease in all electron wave energies, leading to smaller band gaps.

Polymer Semiconductors

Organic polymers are chain molecules comprising a repeating set of "monomers" (which are organic molecules). The electron wavefunctions of neighbouring atoms merge into delocalised states, and the symmetry of these states help define their energetics. If these states are rotationally symmetric about the axis between the neighbouring atoms,

then they have maximally "merged" and so are normally the strongest of delocalised bonds available (called σ-bonds) and as such form the backbone of many polymers.

Consider a carbon atom in its ground state of $[He]2s^2 2p^2$. To bond it with three other groups one of the $2s$ electrons becomes excited to give $[He]2s^1 2p^3$, whereupon the s, p_x and $p_y$states become "hybridised" to give three sp^2 states. Electrons in these states can form σ-bonds to the neighbouring groups, and to maximise the distance between these bonds they all lie in the $x-y$ plane at 120^o intervals. Since the σ-bonds are such strong bonds, they are now lower in energy than the p_z state (which explains why the hybridisation was able to happen). This p_z state protrudes from the $x-y$ plane and is half-occupied, so if this carbon is now in a chain of carbons in the same hybridised state, the p_z states will combine to form a delocalised conjugated system which is half-filled, meaning electrons can move between the atoms inside this conjugated system. Doing so requires the electrons to tunnel between the neighbouring p_z states, which is highly dependent on the distance between the atoms. As such we can predict that the peaks in absorption and PL will be at lower energies as the temperature is increased, since thermal motion along the chain allows for neighbouring atoms to spend more time closer together.

Instead of trying to pass a current through the material, we are optically activating this "hop". We aren't dealing with a continual stream of electrons but the singular hopping to-and-from a neighbouring atom. After hopping to the atom, the structure of the polymer will change such that the energy recovered by hopping back is less than that absorbed in hopping to the atom. We can therefore expect to see a higher-energy peak in absorption than photoluminescence.

2.2 Excitons

So far we have discussed the excitation and relaxation of electrons. A more encompassing approach is to also consider the empty state that the electron leaves behind as a particle itself, called a "hole". This is useful when discussing conductivity, since electrons travel in the highest-occupied state and holes travel in the lowest-unoccupied state, so net conductivity relies on both of these energy levels and is most easily described with this concept whereby the properties of either states are translated into effective masses of the electrons and holes.

Applying this to spectrometry, we see that absorption of a photon by a semiconductor creates an electron-hole pair which eventually recombine to emit a photon. Before recombination, the electron and hole create a hydrogenic system (like positronium, the system of an electron and a positron) which has quantised energy levels. The size of these energy levels determines the exciton type.

Wannier-Mott Excitons

Since crystalline semiconductors have high carrier mobility, electric fields within the material are suppressed (which is quantified by a high dielectric constant). This subdues the electrostatic attraction between the electron and hole in an exciton, giving a formation energy of the order of tens of meV and an expected radius large enough to encompass many lattice points. This reduces the effect of the lattice on the exciton energy levels, allowing us to approximate them with the Bohr model.

Frenkel Excitons

By contrast, carriers in polymer semiconductors are far less mobile and so the electric field between the electron and hole in an exciton is far less screened. This gives a larger exciton formation energy of $100meV - 1eV$.

2.3 Indirect Transitions

Some electronic transitions have momentum and energy requirements that can't be met by a single photon. In such a case, the absorption of the photon must happen together with the absorption of a phonon, or stimulation of an exciton. Similarly on relaxation, the electron might emit both a phonon and a photon.

In the case of a phonon-assisted transition, we can predict that reducing temperature will not affect the spectra until we pass the material's Debye temperature, after which the transition will require more energy to be put into the photon.

2.4 Multi-Quantum Wells (MQW)

In a MQW, a semiconductor is sandwiched between two other semiconductors which have a

larger energy gap. The carrier wavefunctions in the central layer are now confined to the two dimensional plane of the layer.

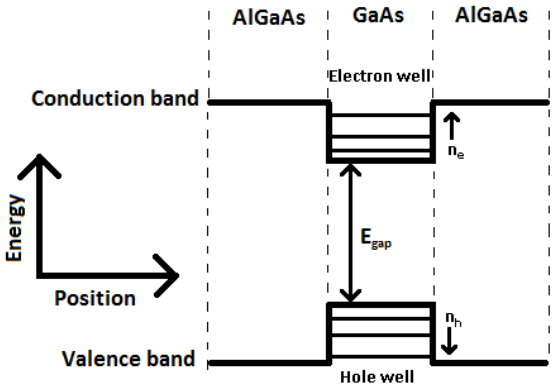

Figure 2.1: Band structure across the semiconductor sandwich

As the figure above shows, a well is created for each carrier type. Upon photo-excitation, an electron-hole pair is created within their respective wells. They will recombine to emit a photon with an energy of E_{gap} plus the energies of the occupied states in each well.

Infinite Potential Well Model

A simplistic model is to assume each well's walls are infinite in potential, whilst each carrier takes on an effective mass not necessarily the same as the effective mass within the semiconductors. In doing so we find that

$$E_{well}(n) = \frac{\hbar^2}{2m^*}\left(\frac{n\pi}{L}\right)^2 \tag{2.1}$$

where n is the quantum number.

So the emitted photon will have energy

$$E_p = E_{gap} + \left(\frac{\hbar\pi}{L}\right)^2\left(\frac{n_h^2}{2m_h^*} + \frac{n_e^2}{2m_e^*}\right)$$

In the creation of a particle-antiparticle pair, momenta is shared equally between the two. This tells us that the momenta of the electron and hole states must be equal, which can only be true if $n_h = n_e$. Therefore,

$$\begin{aligned} E_p &= E_{gap} + \left(\frac{\hbar n\pi}{L}\right)^2\left(\frac{1}{2m_h^*} + \frac{1}{2m_e^*}\right) \\ &= E_{gap} + \frac{1}{2\mu^*}\left(\frac{\hbar n\pi}{L}\right)^2 \end{aligned}$$

where μ^* is the reduced effective mass of the electron-hole pair, given by

$$\frac{1}{\mu^*} = \frac{1}{m_h^*} + \frac{1}{m_e^*}$$

Finite Potential Well Model

The fact that the well is not infinitely deep allows for the carrier's wavefunction to extend beyond the spacial confines of the well. Outside the well (ie. in the AlGaAs) the carriers' masses and energies are different, so the derivation is more involved.

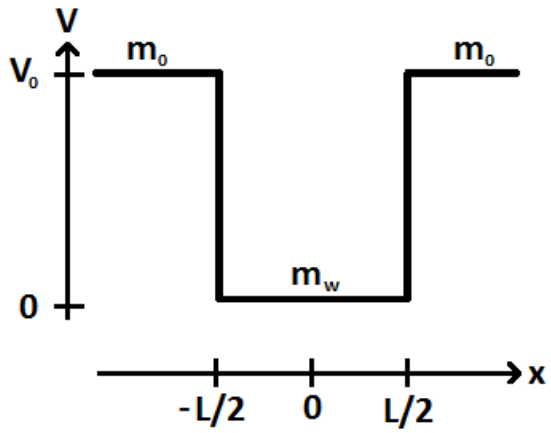

Figure 2.2: A schematic of the finite potential well model

The Hamiltonian is therefore

$$\mathcal{H} = \begin{cases} \frac{p^2}{2m_w} & \text{for } |x| < \frac{L}{2} \\ \frac{p^2}{2m_0} + V_0 & \text{for } |x| > \frac{L}{2} \end{cases}$$

We now apply these to the time-independent Schrödinger equation, $\mathcal{H}\psi = E\psi$. Firstly inside the well:

$$\begin{aligned} -\frac{\hbar^2}{2m_w}\frac{d^2}{dx^2}\psi &= E\psi \\ \therefore \psi'' &= -k_w^2\psi \\ \text{Where } k_w &= \frac{1}{\hbar}\sqrt{2m_wE} \\ \implies \psi &= Ae^{ik_wx} + Be^{-ik_wx} \end{aligned} \tag{2.2}$$

The symmetry of the well in the x axis requires ψ to be either symmetric or antisymmetric, so either $A = B$ or $A = -B$, giving

$$\psi = a \sin k_w x + b \cos k_w x$$

where a and b are real.

Outside of the well,

$$\begin{aligned} -\frac{\hbar^2}{2m_0}\frac{d^2}{dx^2}\psi &= (E - V_0)\,\psi \\ \therefore \psi'' &= k_0^2 \psi \\ \text{Where } k_0 &= \frac{1}{\hbar}\sqrt{2m_0\,(V_0 - E)} \qquad (2.3) \\ \implies \psi &= C_1 e^{k_0 x} + C_2 e^{-k_0 x} \end{aligned}$$

We have chosen $E < V_0$, so the wavefunction must attenuate at large x. Therefore

$$\psi(x) = \begin{cases} C_1 e^{k_0 x} & \text{for } x < -\frac{L}{2} \\ a \sin k_w x + b \cos k_w x & \text{for } |x| < \frac{L}{2} \\ C_2 e^{-k_0 x} & \text{for } x > \frac{L}{2} \end{cases}$$

We may consider the symmetric (cosine) and antisymmetric (cosine) solutions independently due their orthogonality. In the symmetric case, we require $C_1 = C_2$ and in the antisymmetric case we require $C_1 = -C_2$, hence

$$\psi_{sym}(x) = \begin{cases} c e^{k_0 x} & \text{for } x < -\frac{L}{2} \\ b \cos k_w x & \text{for } |x| < \frac{L}{2} \\ c e^{-k_0 x} & \text{for } x > \frac{L}{2} \end{cases}$$

$$\psi_{anti}(x) = \begin{cases} -d e^{k_0 x} & \text{for } x < -\frac{L}{2} \\ a \sin k_w x & \text{for } |x| < \frac{L}{2} \\ d e^{-k_0 x} & \text{for } x > \frac{L}{2} \end{cases}$$

At the boundaries between these regions, the wavefunctions and their derivatives must be continuous. For the symmetric solution at $x = L/2$,

$$\begin{aligned} \psi_{sym}\,(L/2 + \delta) &= \psi_{sym}\,(L/2 - \delta) \\ \therefore c e^{-k_0 L/2} &= b \cos \frac{k_w L}{2} \qquad (2.4) \\ \psi'_{sym}\,(L/2 + \delta) &= \psi'_{sym}\,(L/2 - \delta) \qquad (2.5) \\ \therefore -c k_0 e^{-kL/2} &= -b k_w \sin \frac{k_w L}{2} \qquad (2.6) \end{aligned}$$

Similarly for the antisymmetric solution,

$$\begin{aligned} \psi_{anti}\,(L/2 + \delta) &= \psi_{anti}\,(L/2 - \delta) \\ \therefore d e^{-k_0 L/2} &= a \sin \frac{k_w L}{2} \qquad (2.7) \\ \psi'_{anti}\,(L/2 + \delta) &= \psi'_{anti}\,(L/2 - \delta) \qquad (2.8) \\ \therefore -d k_0 e^{-kL/2} &= a k_w \cos \frac{k_w L}{2} \qquad (2.9) \end{aligned}$$

Dividing equations 2.6 by 2.4 and 2.9 by 2.7 gives

$$\frac{k_0}{k_w} = \begin{cases} \tan \frac{k_w L}{2} & \text{for } \psi_{sym} \\ -\cot \frac{k_w L}{2} & \text{for } \psi_{anti} \end{cases}$$

Using equations 2.2 and 2.3 we can express k_0 and k_w in terms of the carrier energy, E, giving

$$\sqrt{\frac{m_0}{m_w}\left(\frac{V_0}{E} - 1\right)} = \begin{cases} \tan \frac{L\sqrt{2m_w E}}{2\hbar} & \text{for } \psi_{sym} \\ -\cot \frac{L\sqrt{2m_w E}}{2\hbar} & \text{for } \psi_{anti} \end{cases} \qquad (2.10)$$

3 Method

We designed two sample holders to allow for transmission and photoluminescence spectra, as shown in figures 3.1 and 3.2 respectively.

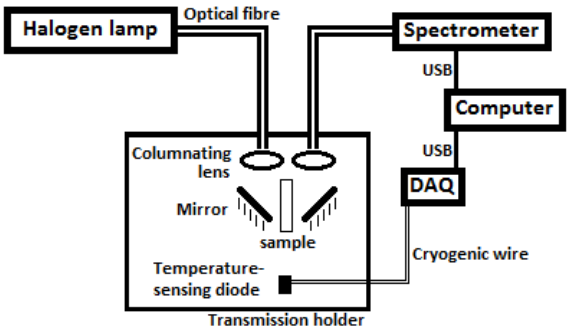

Figure 3.1: Experimental set up for taking transmission spectra

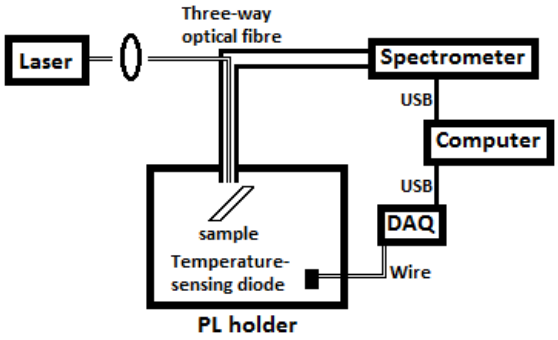

Figure 3.2: Experimental set up for taking PL spectra

We used an Ocean Optics (USB4000) spectrometer, two Lakeshore DT-470 temperature sensing diodes, a Lakeshore DAQ (digital acquisition) device, an Ocean Optics HL-2000-FHSA halogen lamp, and a three-way optical fibre.

We developed software to interface with the DAQ and spectrometer to allow for automated data collection as the sample was cooled, by submersion in liquid nitrogen and then liquid helium (for PL spectra only, since the previous investigator of this project reports that transmission spectra of the samples used do not change between liquid nitrogen and liquid helium temperatures).

Of interest in the PL spectra are the peak energies, so we were able to change the integration time as the sample was cooled to whatever value gave the best peak definition (ie. the largest peaks possible without saturating the spectrometer). For expediency we exported spectra to Origin Lab 8.1 to use its peak fitting tool, and then developed scripts to present the peak energies against sample temperature.

For transmission spectra we instead are interested in the absorption coefficients across wavelengths, λ, of A_λ as defined in [4] by

$$A_\lambda = -\log_{10}\left(\frac{S_\lambda - D_\lambda}{R_\lambda - D_\lambda}\right)$$

where S_λ is the spectrum with the sample in the holder, D_λ is the spectrum with the halogen lamp turned off, and R_λ is the spectrum with the lamp on but the sample removed from the holder. This coefficient allowed us to deduce the energy gaps in crystalline semiconductors using [4]

$$E - E_g \propto \begin{cases} A^2 & \text{for direct transitions} \\ \sqrt{A} & \text{for indirect transitions} \end{cases}$$

The software we developed allowed for these spectra to be algebraically manipulated to show the A_λ spectrum in real-time.

A problem presented itself when taking data because, as the sample was cooled and the spectral peaks grew in size, we needed to decrease the integration time to avoid saturating the spectrometer, but the R_λ spectrum would only have been taken at the starting integration time. The software was therefore improved to allow for the integration time of the sample being recorded to be a variable in the equation of A_λ, allowing the R_λ and D_λ spectra to be scaled according to the integration time.

4 Observations

4.1 Polymer Semiconductor - PFO

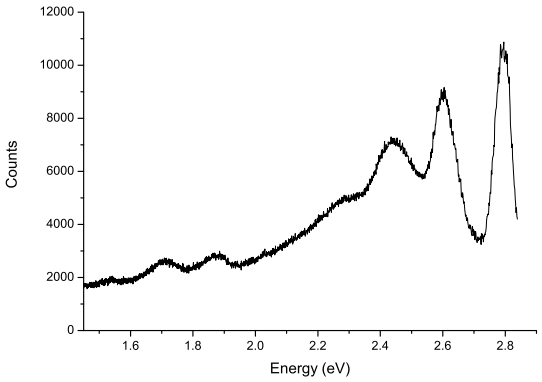

Figure 4.1: PFO PL spectrum (6K)

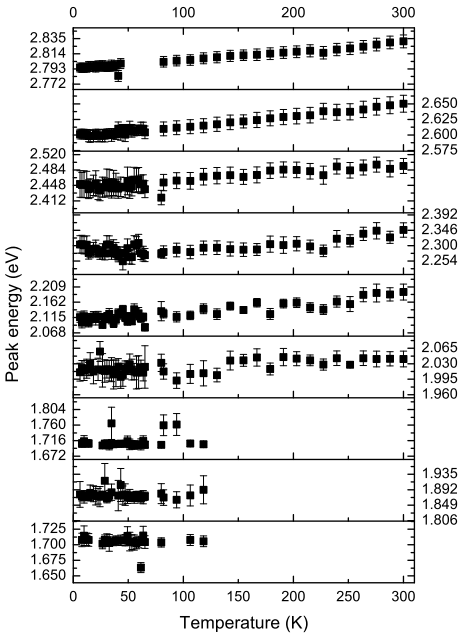

Figure 4.2: PFO PL spectral peaks' energies

4.2 Multi-Quantum Wells

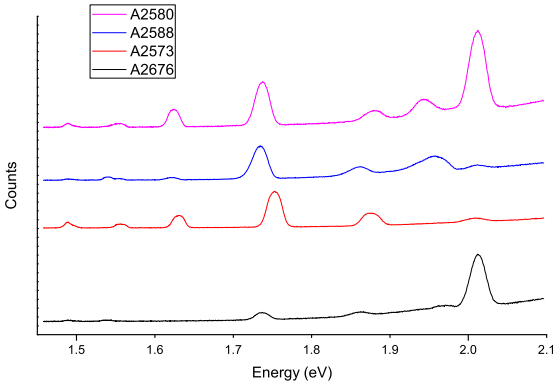

Figure 4.3: PL spectra for four MQW samples (6K)

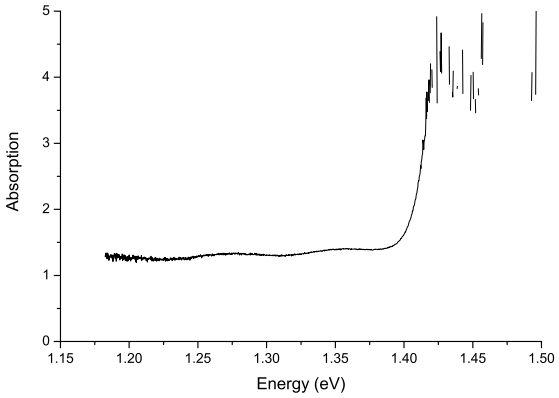

Figure 4.5: Absorption spectrum of GaAs

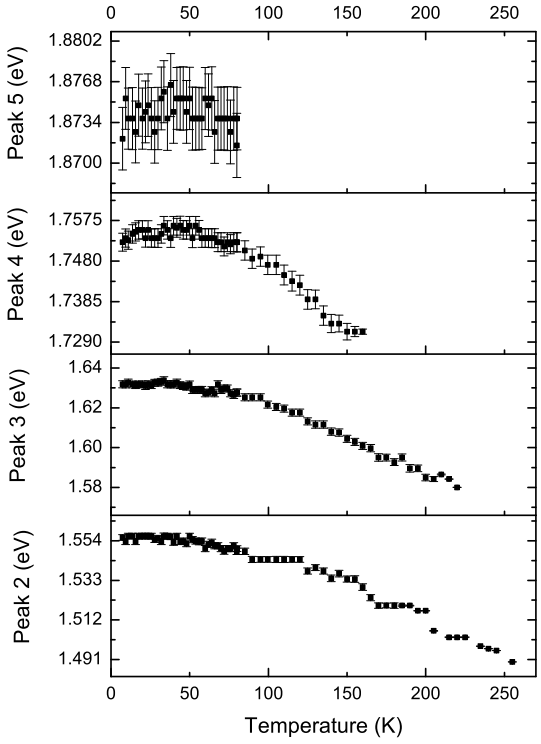

Figure 4.4: PL spectral peaks' energies for sample A2573

4.3 Crystal Semiconductor - GaAs

5 Analysis

5.1 Polymer Semiconductor - PFO

As temperature decreases, we see that the largest peak decreases in energy, meaning the energy released as an electron to hop within the π conjugate system decreases. This could be explained by the polymer contracting as it cools, shortening the distance between neighbouring p_z orbitals (ie. the distance between the electron and its hole), thus reducing the exciton's energy which is released on recombination.

Subsequent peaks come from phonon-assisted transitioning. They are of a similar amplitude, confirming that phonons are plentiful in the molecular bonds. The difference between the first and subsequent peaks gives the energies of the phonons involved.

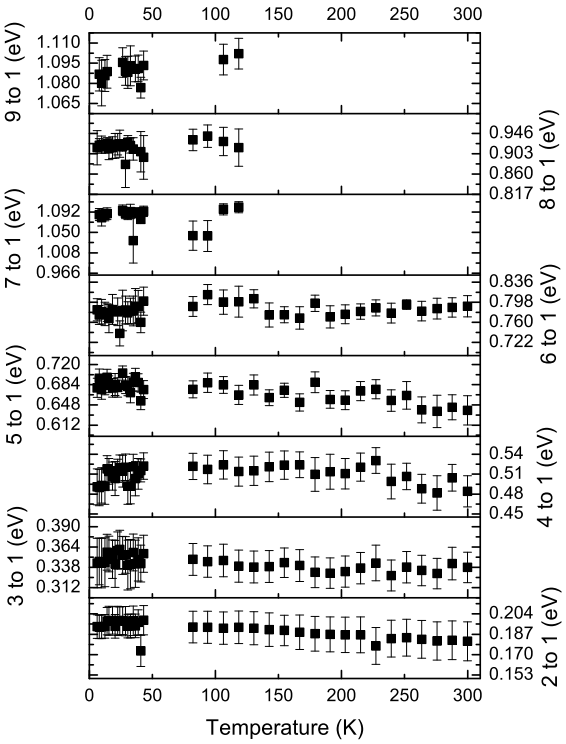

Figure 5.1: Difference in energy between the first and subsequent PL peaks of PFO

These energies are almost constant with respect to temperature (within error boundaries). The averages of these energies are shown below.

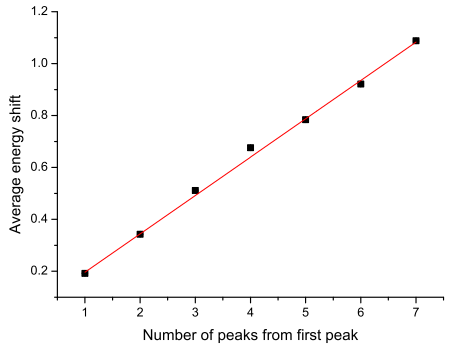

Figure 5.2: Plot an linear fit of relative peak number and energy shift from first peak

As shown, the average energy between peaks and the first peak increases almost linearly. The line has an intercept of 0.048 ± 0.009 eV, and a slope of 0.147 ± 0.003 eV/peak. This suggests an average phonon energy of 0.147 ± 0.003 eV, with these subsequent peaks arising from multiple phonons being produced from each electron-hole recombination.

With this in mind we need only consider the temperature dependence of the first peak, which we do first by comparison with the Varshni [1] empirical equation,

$$E(T) = E(0) - \frac{\alpha T^2}{T + \beta}$$

We find $\alpha = (-1.30 \pm 0.15) \times 10^{-4}$eV/K, $\beta = 37.7 \pm 37.1$K, and $E(0) = 2.794 \pm 0.001$ eV.

5.2 MQW - Sample 2573

This sample contains four types of well with widths 1.2nm, 2.5nm, 5nm, and 10nm. We expect therefore to find a peak for each type of well, and two peaks for the band gaps in the GaAs and AlGaAs. Equation 2.1 tells us that larger well widths refer to lower-energy peaks, so we can assign the peaks to their widths (with the AlGaAs peak representing a zero-width well) and make a plot.

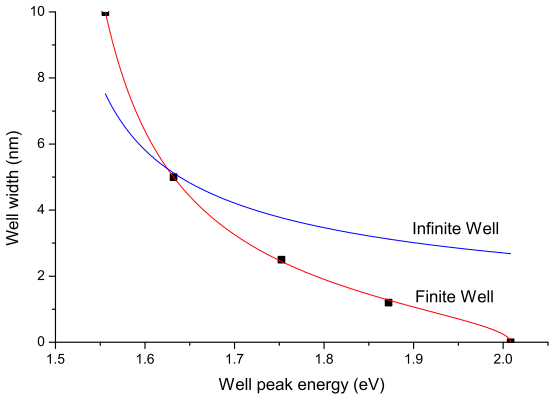

Figure 5.3: Plot of well width against $n = 1$ energy

We have fitted the infinite and finite models from equations 2.1 and 2.10 respectively, taking $n = 1$ in all cases. Clearly only the finite potential well model is more appropriate than the infinite potential well model.

An attempt was made to fit the more realistic model of a pair of finite wells as described in figure 2.1, but this required four parameters (ie. the masses of each charge carrier both inside and outside the well) to be determined from a dataset of only five points, which led to an unsatisfactory fit. Instead, the electron mass represents something similar to a reduced mass between the electrons and holes. The fit gave the mass outside the well as $m_0/m_e = (3.97 \pm 0.59) \times 10^{-3}$ and inside the well as $m_0/m_e = (1.81 \pm 0.10) \times 10^{-2}$ where m_e is a free electron's rest mass.

All the peaks had the same temperature dependence, originating from the change in lattice (and therefore well) size as temperature changes. Fitting the second peak (relating to the 10nm well) to the Varshni empirical formula gives $\alpha = (1.19 \pm 0.56) \times 10^{-4} JK^{-2}$, $\beta = (900 \pm 580)K$, and $E(0) = (1.5576 \pm 0.0025)eV$.

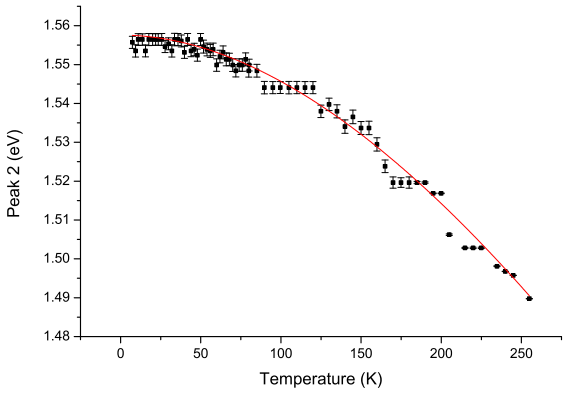

Figure 5.4: Temperature dependence of a QW's $n = 1$ energy level.

5.3 Crystal semiconductor

GaAs

Since we know that a direct semiconductor will have a quadratic relation between absorption and photon energy, we plot A^2 against photon energy and perform a linear fit to the sharp rise in the $1.3 \rightarrow 1.42$ eV region. From previous data [2] we know that the photon energy with $A = 3.06$ is 10 ± 3meV below the band gap, so we interpolate using the linear fit then add 10 ± 3meV, giving figure

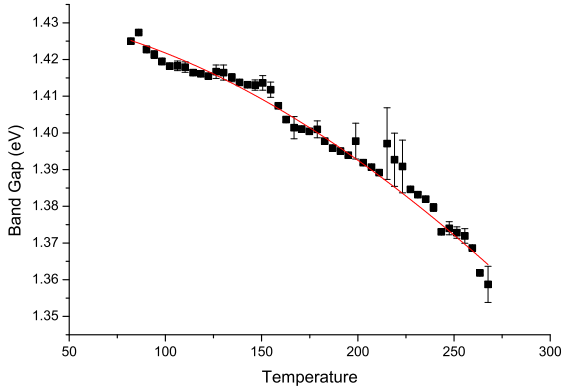

Figure 5.5: Temperature dependence of the band gap energy in GaAs.

Where the line is the fitted Varshni equation, with parameters of $\alpha = (1.47 \pm 0.9) \times 10^{-3}$ eV/K, $\beta = 1273 \pm 959$K, and $E(0) = 1.43249 \pm 0.013$eV.

The band gap energies calculated are approximately 0.09eV lower than the value reported in the literature, where $E(294) = 1.435 \pm 0.003$ eV [2] and $E(77) = 1.512 \pm 0.001$eV [3]. Absorption data collected on GaAs last year using this same methodology attains better values, and there are discrepancies between that data and the data collected here. It is possible that the sample we used had impurities, and had time allowed we would have repeated our analysis on other GaAs samples.

6 Conclusion

We have demonstrated a range of physical phenomena with only an inexpensive laser, lamp and spectrometer, and developed a lab script and software to aid future students in using the set up to further their understanding of these phenomena.

We found that the MQW spectra were most useful at low temperatures, where thermal broadening was reduced. However the spectra at liquid helium temperatures were very similar to those at 16K, which is achievable using a cold finger with far fewer practical difficulties. As such we'd recommend integrating the sample holder used for photoluminescence into a cold finger in future.

We were able to fit the MQW peaks to a simplified version of the finite potential well model, but in doing so were only able to prove the model was valid without using the model to estimate charge carrier masses. To fit the more complete model we would need more data points, which could be accomplished by producing MQWs of different sizes - a possible avenue of future research.

7 Acknowledgements

My thanks go to Mr Peter Schrimpton, Mr Mohammed Cheddi and Mr Jeffrey Lidgard for all of their help and patience, Mr Keith Long for manufacturing and modifying the sample holders, and Professor Robin Nicholas for his invaluable guidance and support.

References

[1] Y. P. Varshni, Physica (Amsterdam) 34, 149 1967

[2] M.D. Sturge Phys. Rev. 127, 768773 (1962)

[3] E. Grilli, M. Guzzi, L. Pavesi and R. Zamboni Phys. Rev. B 45, 16381644 (1992)

[4] Mark Fox, Optical properties of solids, OUP 2001

[5] P. Acosta-Díaz, O. Cano-Aguilar and F.L. Castillo-Alvarado, Superficies y Vacío 12, 39-44

Appendix - Introduction

This script aims to demonstrate how visible-light spectroscopy can be used to investigate semiconductors. We will use transmission spectra to determine the energy gaps in a crystalline semiconductor, then photoluminescence (PL) spectra to understand how phonons affect electron transitions in a range of semiconductors. Lastly we use PL spectra to study the energy levels in quantum wells using both the infinite and finite potential well models. Throughout the experiment we'll monitor the temperature-dependence of the aforementioned phenomena.

[Answers to questions posed in the script are written like this, and should not be given to students]

1 Semiconductor Theory

A key property of a semiconductor is that a small yet finite gap exists between the highest-energy occupied electron state and the lowest-energy unoccupied electron state. This gap can have the energy of a visible-range photon, so a visible-light source can be used to excite outer electrons to transition between these states, then a visible-light spectrometer can be used to measure transmission or PL from the material. It is the ease with which electron transitions can be controlled which makes semiconductors ideal for this experiment, since we can be certain that we are only activating one transition. This would be in contrast to, for example, X-ray spectrometry which would activate a variety of transitions and could complicate data analysis.

1.1 Crystalline Semiconductors

In a crystalline semiconductor, the electrons occupy delocalised wavefunctions which are distributed throughout the material. These wavefunctions are similar to a free-electron wavefunction because (semi-classically) a nucleus on an electron's left will attract it almost as much as the nucleus on its right. Putting a free-particle in an infinite-potential well and applying the relevant boundary condition is all that's required to quantise the possible wavefunctions - similarly, putting a free-electron in a periodic potential applies a condition on the available wavefunctions which leads to quantisation. It is slightly different here since the potential is weak instead of infinite (so the electrons retain a free-electron-like wavefunction) and the boundary condition is periodic instead of being confined to a well (so the allowed k-states relate to having the wavefunction match up to the lattice structure). Similar k-states of different magnitude form a continuous band of states, which can have a finite difference in energy to other bands known as the band gap energy. In a semiconductive crystal this is a few eV and so the electrons in the highest-energy band will be excited by visible-light photons.

1.2 Polymer Semiconductors

Organic polymers are chain molecules comprising a repeating set of "monomers" (which are organic molecules). The electron wavefunctions of neighbouring atoms merge into delocalised states, and the symmetry of these states help define their energetics. If these states are rotationally symmetric about the axis between the neighbouring atoms, then they have maximally "merged" and so are normally the strongest of delocalised bonds available (called σ-bonds) and as such form the backbone of many polymers.

Consider a carbon atom in its ground state of $[He]2s^2 2p^2$. To bond it with three other groups one of the $2s$ electrons becomes excited to give $[He]2s^1 2p^3$, whereupon the s, p_x and $p_y$states become "hybridised" to give three sp^2 states. Electrons in these states can form σ-bonds to the neighbouring groups, and to maximise the distance between these bonds they all lie in the $x-y$ plane at 120^o intervals. Since the σ-bonds are such strong bonds, they are now lower in energy than the p_z state (which explains why the hybridisation was able to happen). This p_z state protrudes from the $x-y$ plane and is half-occupied, so if this carbon is now in a chain of carbons in the same hybridised state, the p_z states will combine to form a delocalised conjugated system which is half-filled, meaning electrons can move between the atoms inside this conjugated system. Doing so requires the electrons to tunnel between the neighbouring p_z states, which is highly dependent on the distance between the atoms. As such we can predict that the peaks in absorption and PL will be at lower energies as the temperature is increased, since thermal motion along the chain allows for neighbouring atoms to spend more time closer together.

Instead of trying to pass a current through the ma-

terial, we are optically activating this "hop". We aren't dealing with a continual stream of electrons but the singular hopping to-and-from a neighbouring atom. After hopping to the atom, the structure of the polymer will change such that the energy recovered by hopping back is less than that absorbed in hopping to the atom. We can therefore expect to see a higher-energy peak in absorption than photoluminescence.

1.3 Phonons

A phonon is a quasiparticle which embodies the emergent properties of a wave of vibration in a system. They are the quantum equivalent to the wave solutions of the normal modes in a system of masses interconnected by springs. As in this classical scenario, there are phonons where neighbouring atoms either move in opposing directions (called "optical" phonons) or similar directions (called "acoustic" phonons). Acoustic phonons carry sound waves, and at large wavevectors the energy and wavevectors of the phonons are linearly related.

Optical phonons have non-zero energy at zero wavevector (ie. when atoms in a chain connected by springs move exactly oppositely to its neighbours, there is no net transfer of energy yet there is energy stored in the vibrational mode). This is similar to photon, which has a comparatively minute wavevector and a finite energy. This means photons can be absorbed by the structure in creating an optical phonon, hence their name.

1.4 Direct and Indirect Transitions

Some electronic transitions have momentum and energy requirements that can't be met by a single photon. In such a case, the absorption of the photon must happen together with something else such as the absorption of a phonon. Similarly on relaxation, the electron might emit both a phonon and a photon. Either case is called an indirect transition. Depending on the material's structure, there may be multiple combination of available phonons which allow photons of various energies to cause a transition. As such an indirect semiconductor will normally show more spectral peaks than a direct semiconductor.

2 Transmission Spectra

In relating transmission spectra to energy gaps, we are interested in the absorption spectrum A as defined by

$$A = -\log_{10}\left(\frac{S-D}{R-D}\right)$$

where S is the spectrum with the sample in the holder, D is the spectrum with the halogen lamp turned off, and R is the spectrum with the lamp on but the sample removed from the holder. This spectrum allows us to deduce the energy gap E_g in a crystalline semiconductor using

$$E - E_g \propto \begin{cases} A^2 & \text{for direct transitions} \\ \sqrt{A} & \text{for indirect transitions} \end{cases} \quad (2.1)$$

where E is the energy of the incident photon. Assuming the band gap is sufficiently described by the absorption spectrum, one can find E_g by plotting E against either A^2 or $\sqrt{A}$, then by extrapolating the steepest rise linearly down to the intersection with $A = 0$. The energy at this intersection will be E_g.

2.1 Initial Set Up

Ensure the equipment is set up as in figure 3.1.

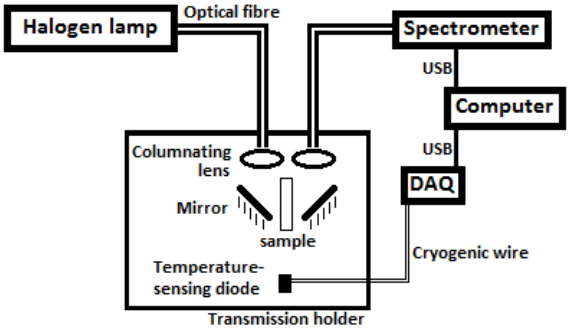

Figure 3.1: Experimental set up for taking transmission spectra

Light is focussed from the halogen lamp into the optical fibre, columnated by the first lens, is passed through the sample, focussed into the second optical fibre, then detected by the spectrometer. The sleeves into which the fibres screw in the sample holder can move toward or away from the lenses by loosening the relevant grub screw. By screwing the optical fibre from the lamp into each sleeve in turn, adjust the sleeve's height until the light bouncing

off the attached mirror is columnated. *Hint - be sure the grub screws are properly tightened.*

'TrAPS' is a piece of software developed specifically for this experiment. Run it and click the 'Change curve' button then find 'transmission_temp_calib.dat'. This contains the calibration data required to convert the voltage across the temperature-sensing diode mounted on the sample mount as measured by the DAQ into a temperature (shown at the bottom-left of the computer screen).

2.2 Room Temperature Absorption Spectrum

For this section we are concerned with the absorption scale defined in equation 2.1, for which we need a background and a reference spectrum. Rename the current dataset name as "background", then with no sample in the holder and the halogen lamp turned off click "Aquire". Now to the right of the dataset name box click the '+' button to add a new dataset, and rename this as 'reference'. Turn the lamp on and open the aperture as far as possible without the spectrometer becoming saturated. *Hint - tap the lamp to make sure the aperture won't wriggle open, since we need it to stay at its current size.* Click 'Aquire'.

To show the absorption scale on the graph, click the 'Add View' button beneath the graph and type '`-log((live-background)/(reference-background))`' into the equation column and 'absorption' as the name for the new view. Create another view called 'scaled_abs' with the equation 'absorption*1e5'; the factor of $10^5$is to allow for both the absorption and transmission spectra to be seen simultaneously. This will become important later.

Put the GaP sample into the holder. Why does the absorption spectrum become fuzzy at the extremes of photon energy? *Hint - look at the reference spectrum and equation 2.1.*

[The halogen light doesn't emit much light in those ranges, so 'reference-background' is small, so any small perturbation in the live spectrum becomes larger]

2.3 Integration Time

The sample has caused the entire spectrum to attenuate. To compensate for this the integration time of the spectrometer can be increased using the box in the top-left of the screen, thus increasing the number of photons detected in all wavelengths. Soon we will need to compare spectra captured with different integration times, which becomes difficult if the spectral amplitudes are arbitrary with respect to each other. To simplify this, the software automatically scales the collected spectra to have amplitudes as if it were captured using the lowest integration time, $3.8ms$. In practice, this means that increasing the integration time will not increase the spectral amplitudes but instead decrease the saturation amplitude, shown on the graph as a grey horizontal line starting at around 65000 counts. To maximise accuracy one must maximise the integration time whilst keeping the live view's spectrum below the saturation amplitude.

2.4 Room Temperature Energy Gap

Create a view with the equation 'sqrt(absorption)' then right-click on it and select 'export', choosing somewhere appropriate to place the file, then open Origin Lab and import it. Plot the data as a line graph and recall that we are only conscerned with the steepest linear section of the spectrum. To this end open the 'Gadgets' menu and select 'Cluster', which allows you to manipulate data inside a graph. Resize the rectangle until only the linear section is contained, then mask everything outside the rectangle, which will turn red if successful. Extrapolate this linear section to find the energy at $\sqrt{A} = 0$, which is the energy gap in GaP. Check your value with a demonstrator, then ask for some liquid nitrogen.

2.5 Temperature-Dependent Energy Gap

On the left of the TrAPS window check the 'Trigger by temperature' box. Set the maximum temperature to 300K, the minimum to 75K, and choose to take 40 spectra. Create a new dataset called 'GaP' and click 'aquire', then edit the 'absorption view' equation by replacing 'live' with 'GaP'. Hide all but the square-rooted-absorption and live views by unchecking them. You should see on the graph the live transmission spectrum (to maximise accuracy as per section 3.1.3) and every time the temperature drops past a grey marker a spectrum will be taken and converted to an square-rooted-absorption spectrum on the graph. Put the sample holder in the nitrogen container so it only

just touches the liquid. Why should this matter? Wait until the temperature settles around 77K. If you find the amplitudes change wildly try pushing cryogenic putty into the joints between the mirrors and the holder and try again.

[Nitrogen bubbles cause the spectra to change amplitude very quickly; the slower the holder cools down, the more similar the diode and the sample's temperatures are]

If TrAPS is still in aquiring mode, click 'Stop Aquiring'. Remove the sampel holder from the container to warm up, and watch the live spectrum. Why are we not taking spectra as the sample warms up?

[Reflection from condensation is evident on spectrum; it takes far more time]

Export the square-rooted-absorption view to Origin and follow section 3.1.4, but this time performing a batch-extrapolation to $\sqrt{A} = 0$. This can be done by creating a fitting-function where one of the parameters is the energy gap, then by following the Origin Lab tutorial on batch processing. By making the 'Dataset identifier' the 'Comments' field in the batch processing dialogue, each spectrum's temperature will be used to identify it in the final worksheet.

In Origin, create a new worksheet with two columns (set as X and Y) and fill both with row-numbers. Highlight both rows and press 'control+y', then create a new function, $y = (x - E)/m$, and fit the data to it. In the 'FitNL1' worksheet copy both the value and error for E. Create a new worksheet called 'Output' with two columns ('Energy Gap' set as 'Y' and 'Error' set as 'yErr') then 'paste link' into column 1, row 1. You can now save this as an analysis template, which can be used in the batch processing dialogue.]

Plot temperature against energy gap then fit against Varshni's empirical equation,

$$E(T) = E(0) - \frac{\alpha T^2}{T + \beta}$$

where α, β and $E(0)$ are constants to be found. What are their dimensions? Make a guess as to the physical significances of β and $E(0)$.

[α has units J/K^2; β has units K and relates to the Debye temperature (below which there isn't enough thermal energy to activate all available phonon modes); $E(0)$ is the theoretical band gap energy at absolute zero].

3 Photoluminescence Spectra

Using a 400nm laser we can excite electrons over the band gap and observe the transitions they return by. Each transition involves emitting one photon which we measure, and then by comparison to the band gap energy we can determine the energy spent elsewhere (for example in creating a phonon). As such we are only concerned with the energies of the spectral peaks relating to these photons.

3.1 Initial Set Up

Ensure the equipment is set up as in figure 4.1.

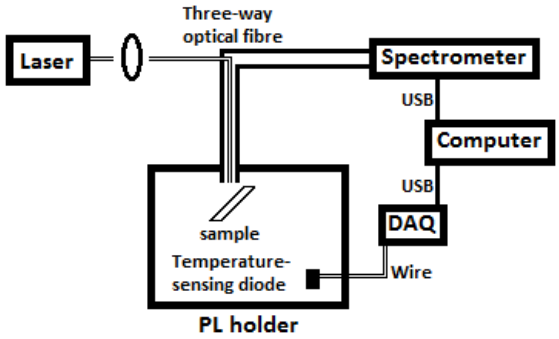

Figure 4.1: Experimental set up for taking PL spectra

The laser light is focussed into the optical fibre and is then absorbed by the sample, which is positioned at an angle so reflected light does not return along the fibre. The sample will photoluminesce at all angles equally (ie. regardless of the angle of the incident light) meaning the photoluminescent light will return via the outer sections of the optical fibre to the spectrometer.

Secure the sample in the mount using cryogenic putty, then close the mount. To maximise the returned light have TrAPS show the live spectrum whilst moving the three-way fibre relative to the sample and changing the distance from the lens to the optical fibre.

3.2 Data Collection

Talk to a demonstrator before cooling the sample. As before, create a new dataset and configure TrAPS to collect spectra across a range of temperatures, this time down to 4K. Decreasing the sample's temperature slowly will, again, increase accuracy of the recorded temperatures. Export the data to Origin.

3.3 Peak Detection

Given the amount of noise in the spectra, setting up automated peak detection means finding the settings which will detect all the true peaks and a minimum of false peaks. Use Origin's 'Peak Analysis' tool and pay attention specifically to the peak finding and filtering settings. The FFT Filter with a cut-off frequency of 0.01 is a good starting point. After testing the settings with a selection of spectra to ensure it will work for all temperatures, save the dialogue theme from inside the peak analyser. Then use the 'Batch Peak Analyser' with the dialogue theme to find all peaks throughout the range of spectra, making the dataset identifier the 'Comments' again.

Make a scatter plot of temperature against peak energy and open the cluster gadget. In its preferences/calculation pane check 'Indices' and uncheck everything below. Select groups of peaks (ie. the same peak which slowly changes with temperature) in turn, each time clicking 'Output Statistics Report'. This puts each group of peaks into a column by reference to the row index in the original peak energies worksheet. Now use the custom-written 'Make peaks summary' script in the analysis menu to create a worksheet containing peak energies and errors, and another containing the difference between these energies (with errors).

3.4 Peak Analysis

What relation is there between the differences between peak energies? *[They are all very similar].* Why are there so many peaks? *[Tunnelling between adjacent p_z states along a polymer chain is highly dependent on the distance between the monomers, which is highly dependent on phonons].* Fit the highest-energy peak to the Varshni empirical formula.

4 Quantum Wells

4.1 Theory

In a MQW, a semiconductor is sandwiched between two other semiconductors which have a larger energy gap. The carrier wavefunctions in the central layer are now confined to the two dimensional plane of the layer.

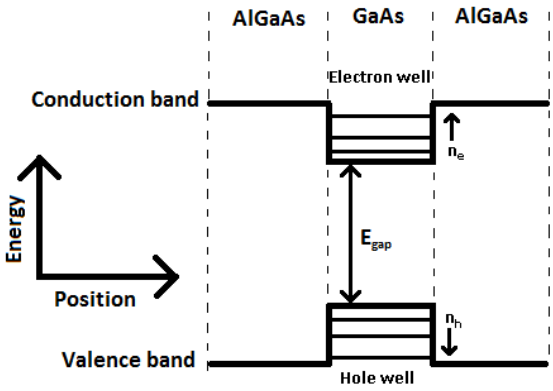

Figure 5.1: Band structure across the semiconductor sandwich

As the figure above shows, a well is created for each carrier type. Upon photo-excitation, an electron-hole pair is created within their respective wells. They will recombine to emit a photon with an energy of E_{gap} plus the energies of the occupied states in each well.

Infinite Potential Well model

A simplistic model is to assume each well's walls are infinite in potential, whilst each carrier takes on an effective mass not necessarily the same as the effective mass within the semiconductors. In doing so we find that

$$E_{well}(n) = \frac{\hbar^2}{2m^*}\left(\frac{n\pi}{L}\right)^2 \tag{4.1}$$

where n is the quantum number.

So the emitted photon will have energy

$$E_p = E_{gap} + \left(\frac{\hbar\pi}{L}\right)^2\left(\frac{n_h^2}{2m_h^*} + \frac{n_e^2}{2m_e^*}\right)$$

In the creation of a particle-antiparticle pair, momenta is shared equally between the two. This tells us that the momenta of the electron and hole states must be equal, which can only be true if $n_h = n_e$. Does this mean that a photon can never be absorped and result in $n_h \neq n_e$? *[In our model, this isn't possible. However the real world is more complex than this model, and such a transition can take place - but probably much less often than one where $n_h = n_e$].*

Therefore,

$$
\begin{aligned}
E_p &= E_{gap} + \left(\frac{\hbar n\pi}{L}\right)^2 \left(\frac{1}{2m_h^*} + \frac{1}{2m_e^*}\right) \\
&= E_{gap} + \frac{1}{2\mu^*}\left(\frac{\hbar n\pi}{L}\right)^2
\end{aligned}
$$

where μ^* is the reduced effective mass of the electron-hole pair, given by

$$
\frac{1}{\mu^*} = \frac{1}{m_h^*} + \frac{1}{m_e^*}
$$

Finite Potential Well model

The fact that the well is not infinitely deep allows for the carrier's wavefunction to extend beyond the spacial confines of the well. Outside the well (ie. in the AlGaAs) the carriers' masses and energies are different, so the derivation is more involved.

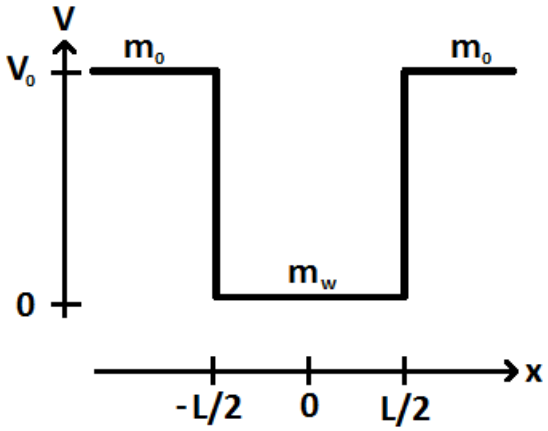

Solutions for the energy allowed levels can only be found numerically from equation 4.2

$$
\sqrt{\frac{m_0}{m_w}\left(\frac{V_0}{E} - 1\right)} = \begin{cases} \tan \frac{L\sqrt{2m_w E}}{2\hbar} & \text{for } \psi_{sym} \\ -\cot \frac{L\sqrt{2m_w E}}{2\hbar} & \text{for } \psi_{anti} \end{cases} \tag{4.2}
$$

4.2 Data Collection

Put sample A2576 into the PL sample holder, then perform the same steps as in section 4.1, 4.2 and 4.3.

4.3 Peak Analysis

The A2573 sample contains four types of quantum well, each with its own width (from 10nm, 5nm, 2.5nm, and 1.2nm). Which other peaks should be present? *[AlGaAs at 2eV and GaAs at 1.49eV]* If the well widths were somehow shrunk to zero, which of these six peaks would remain? *[AlGaAs]*

Try to match the well widths to the PL peak energies (*hint: look at the relationship between E and L in equation 4.1).* Plot peak energy against well width, then using Origin's non-linear function fitter create a fitting function for both the infinite and finite potential well models. (*Hint: find L as a function of E in both equations 4.1 and 4.2).*